

# Potent hypocholesterolemic activity of novel ureido phenoxyisobutyrate correlates with their intrinsic fibrates potency and not with their ACAT inhibitory activity

Roy L. Hawke,<sup>1,\*</sup> James M. Chapman,<sup>†</sup> Deborah A. Winegar,<sup>2,\*</sup> Jo A. Salisbury,<sup>3,\*</sup> Richard M. Welch,<sup>\*</sup> Alan Brown,<sup>3,\*</sup> Karl W. Franzmann,<sup>§</sup> and Carl Sigel<sup>\*</sup>

Division of Pharmacokinetics and Drug Metabolism,<sup>\*</sup> Wellcome Research Laboratories, Research Triangle Park, NC 27709; Department of Basic Pharmaceutical Sciences,<sup>†</sup> College of Pharmacy, University of South Carolina, Columbia, SC 29208; and Department of Medicinal Chemistry,<sup>§</sup> Wellcome, Laboratories, Beckenham, UK

**Abstract** The hypocholesterolemic activity for novel ureido fibrates analogues was found to be over 100-fold greater than for any "second-generation" fibrate in cholesterol-fed rats. A comparison of 12 related analogues revealed that the optimal configuration for a urea-bridging region located between two aromatic rings consisted of a trisubstituted nitrogen, optimally substituted with a C<sub>7</sub> alkyl chain and linked by dimethylene to a phenoxyisobutyrate moiety found in most fibrate analogues. The hypocholesterolemic potency of these compounds was found to correlate with their increased intrinsic fibrate activity as determined by the ability to induce  $\omega$ -hydroxylase activity either in rat hepatocyte cultures or in vivo, and not with their 10-fold increased ACAT inhibitory potency when compared to other fibrates. The most active compound, 2-(4-(2-(N'-(2,4-difluorophenyl)-N-heptylureido)ethyl)phenoxy)-2-methylpropionic acid, referred to as (**2**), was found to induce  $\omega$ -hydroxylase activity in hepatocytes at concentrations between 5 and 100 nM compared to 1–20  $\mu$ M concentrations for bezafibrate, and lower serum VLDL + LDL cholesterol in rats at doses between 0.1 and 0.5 mg/kg per day compared to doses of 25–100 mg/kg per day for bezafibrate. Single-dose pharmacokinetic studies with **2** indicated that total drug exposure will be much lower at hypocholesterolemic doses due to the enhanced intrinsic activity, and may result in an improved safety profile for these novel trisubstituted ureido fibrate analogues in rats and humans compared to other fibrates.—**Hawke, R. I., J. M. Chapman, D. A. Winegar, J. A. Salisbury, R. M. Welch, A. Brown, K. W. Franzmann, and C. Sigel.** Potent hypocholesterolemic activity of novel ureido phenoxyisobutyrate correlates with their intrinsic fibrate potency and not with their ACAT inhibitory activity. *J. Lipid Res.* 1997. **38**: 1189–1203.

**Supplementary key words** fibrates • acyl-CoA:cholesterol acyltransferase •  $\omega$ -hydroxylase • hepatocytes • VLDL + LDL cholesterol

Hypercholesterolemia is now considered a major risk factor in the development of premature atherosclerosis.

Past efforts to slow or even reverse this disease process have focused almost exclusively on the development of potent hypocholesterolemic agents. As a result of these efforts, several classes of hypolipidemic agents are now available for the control of hypercholesterolemia. These include the most recent class of agents, the HMG-CoA reductase inhibitors (1), the second generation fibric acid derivatives (2), and the bile acid sequestrants (3). These various agents can be separated on the basis of their different mechanisms of action, and the combination of cholesterol-lowering drugs from different classes represents a currently accepted therapy for aggressive cholesterol-lowering therapy.

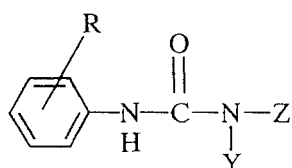
In recent years attention has been given to the development of agents that might possess direct acting anti-atherosclerotic activity in addition to the indirect effects resulting from hypocholesterolemic activity (4). For example, probucol is a unique hypocholesterolemic agent that may have additional antiatherosclerotic activity because of its ability to function as an antioxidant in the arterial wall (5). Another area of pharmaceutical inter-

Abbreviations: ACAT, acyl-CoA:cholesterol acyltransferase; B.I., bezafibrate index; PPAR, peroxisomal proliferator activated receptor; **2**, 2-(4-(2-(N'-(2,4-difluorophenyl)-N-heptylureido)ethyl)phenoxy)-2-methylpropionic acid; CYP4A1, cytochrome P450 4A1  $\omega$ -hydroxylase.

<sup>1</sup>To whom reprint requests should be addressed at: The University of North Carolina at Chapel Hill, School of Pharmacy, CB#7360, Beard Hall, Chapel Hill, NC 27599-7360.

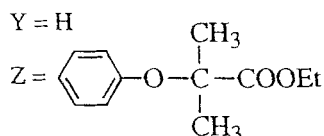
<sup>2</sup>Present address: Department of Metabolic Diseases, Glaxo Wellcome Research and Development, Five Moore Drive, Research Triangle Park, NC 27709.

<sup>3</sup>Present address: Department of Bioanalysis and Drug Metabolism, Glaxo Wellcome Research and Development, Five Moore Drive, Research Triangle Park, NC 27709.

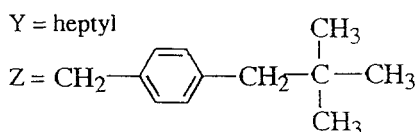


ACAT Inhibitory  
Activity,  $IC_{50}$  ( $\mu$ M)

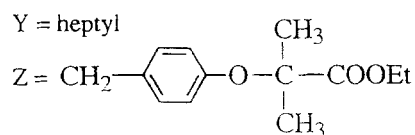
LR-16 where R = 3,4-Cl 30.8



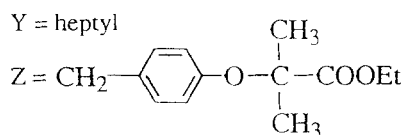
CL277,082 where R = 2,4-F 0.3



BW-USC-209 where R = 3,4-Cl 5.4



BW-USC-148 where R = 2,4-F 7.2



est for the development of direct acting antiatherosclerotic agents has focused on potent inhibitors of acyl-CoA:cholesterol acyltransferase (ACAT, EC 2.3.1.26) activity (6, 7). ACAT-dependent cholesterol esterification is thought to play an important role in the intestinal absorption of cholesterol, in hepatic VLDL synthesis and/or secretion, and in the formation of foam cells and fatty streaks in the arterial wall that are indicative of the early stages of atherosclerosis (8). It has been hypothesized that the inhibition of cholesterol esterification in the arterial wall would decrease foam cell formation and generate free cholesterol which would then be available for removal by HDL (9, 10). Recent studies in cholesterol-fed rabbits have demonstrated direct antiatherosclerotic effects in the arterial wall that were independent of the indirect antiatherosclerotic activity

resulting from decreases in serum cholesterol (11, 12). While several studies in cholesterol-fed animals have shown that ACAT inhibitors have potent hypocholesterolemic activity as a result of an inhibition of cholesterol absorption (13–16), studies with either Lederle's prototypical trisubstituted ureido ACAT inhibitor, CL277,082 (see Fig. 1) (17), or another more potent inhibitor, DuP 128 (18), have found only minimal effects on either cholesterol absorption and excretion rates or on serum cholesterol concentrations in man. Therefore, it is likely that ACAT inhibitors would be used in combination with a potent hypolipidemic agent in order to achieve direct and indirect antiatherosclerotic effects resulting from the inhibition of arterial ACAT activity and the lowering of serum cholesterol, respectively. For example, ACAT inhibitors could potentially be used in

**Fig. 1.** Chemical structures and ACAT inhibitory potencies for LR-16, CL277,082, and two related analogues, BW-USC-209 and BW-USC-148. The four compounds were tested for inhibition of ACAT activity using rat hepatic microsomes obtained from cholesterol-fed rats as described in Materials and Methods. In the presence of the DMSO vehicle only, control ACAT activity was  $310 \pm 50$  pmoles/min · mg protein.  $IC_{50}$ s were calculated from concentration-inhibition curves using at least six concentrations assayed in duplicate.

combination with hypolipidemic agents from the fibrate class. Second generation fibric acid derivatives such as bezafibrate and fenofibrate characteristically demonstrate good hypocholesterolemic and hypotriglyceridemic activity as well as a propensity to increase plasma HDL-cholesterol in humans (19). Thus, the combination of an ACAT inhibitor with an agent that increases HDL-cholesterol is a particularly attractive one because of their complementary mechanisms for increasing the net removal of cholesterol from the atherosclerotic lesion. Alternatively, the development of an ACAT inhibitor that incorporated the lipid modifying properties of the fibric acid derivatives might be a particularly effective anti-atherosclerotic agent. The feasibility of such an approach with fibric acid derivatives is suggested by a report that the disubstituted ureidophenoxyisobutyric acid, LR16 (see Fig. 1), demonstrated potent hypocholesterolemic activity in rats (20). In addition, fibrates have demonstrated significant though relatively weak intrinsic ACAT inhibitory activity in isolated rabbit peritoneal macrophages (21).

In a preliminary experiment to determine whether it was possible to incorporate greater ACAT inhibitory activity within a fibric acid derivative, we combined the salient structural features of CL277,082 and LR16 into a single molecule (see additional structures in Fig. 1) and tested it for ACAT inhibitory activity. This initial study revealed a novel trisubstituted ureidophenoxyisobutyric acid series where specific structural modifications resulted in both increased ACAT inhibitory potency and in greater hypocholesterolemic activity in rats. This is the first report of a brief examination of structure-activity relationships where the essential structural features for the potent hypocholesterolemic activity of this novel trisubstituted ureidophenoxyisobutyrate series are identified. To determine what effects these structural modifications may have on the fibrate-like properties of these compounds, analogues were also screened for their inductive effects in primary cultures of rat hepatocytes. Clofibrate and the other fibric acid derivatives evoke specific pleiotropic responses in rat liver that are indicative for this class of hypolipidemics (22). These responses include peroxisomal proliferation and induction of peroxisomal enzyme activities such as the cyanide-insensitive  $\beta$ -oxidation of fatty acids, and induction of non-peroxisomal enzyme activities such as the terminal ( $\omega$ )-hydroxylation of medium chain fatty acids catalyzed by microsomal enzymes from the CYP4A family of cytochrome P450s (23). Our studies revealed that the increased hypocholesterolemic activity of these trisubstituted ureidophenoxyisobutyrate correlated with their respective potencies for inducing fibrate-type effects in hepatocytes, specifically the induc-

tion of lauric acid  $\omega$ -hydroxylase activity in rat liver, and not with their increased ACAT inhibitory activity.

## MATERIALS AND METHODS

### Materials

[1-<sup>14</sup>C]lauric acid (36.3 mCi/mmol) and [1-<sup>14</sup>C]oleoyl-coenzyme A were obtained from Amersham Corp. (Arlington Heights, IL). Sodium laurate, oleoyl-CoA, bovine serum albumin (fraction V), NADPH, dithiothreitol, clofibrate, fenofibrate, and bezafibrate were purchased from Sigma Chemical Co. (St. Louis, MO). Ciprofibrate was a gift from Sterling Drug, Inc. (Rensselaer, NY), and beclobrate was generously provided by Siegfried Pharma (Zofingen, Switzerland). RPMI 1640 culture medium and fetal bovine serum were obtained from GIBCO Laboratories (Grand Island, NY). Coomassie Protein Assay Reagent was purchased from Pierce (Rockford, IL). All organic solvents and other biochemicals were of the highest purity commercially available.

### Novel ureido and amidophenoxyisobutyrate

N-alkyl analogues of bezafibrate (see Table 1), and compounds 1–12 (see Tables 2 and 3) were synthesized at the University of South Carolina (24). All structures were verified by elemental analysis (Atlantic MicroLab Inc., Norcross, GA), NMR (Bruker WH400), and mass spectrometry. **Figure 2** outlines the chemical synthesis of compound **2**, the most potent ureidophenoxyisobutyrate. Carbobenzyloxytyramine (**1**) (25), 42.76 g (0.158 mol), and 10.23 g of 0.182 M KOH were dissolved with warming in 600 ml of absolute ethanol. Ethyl 2-bromoisobutyrate, 32.94 g (0.169 mol) was added and the resulting solution was refluxed for 22 h. After cooling and filtration, the solvent was removed in vacuo; the residue was redissolved in CH<sub>2</sub>Cl<sub>2</sub>, washed with 1 N NaOH, 1 N HCl, and saturated aq. NaCl, and the organic layer was dried over MgSO<sub>4</sub>. Filtration and removal of the solvent in vacuo yielded 33.37 g of crude **II**. **II**, 2.72 g (0.0071 mol) was dissolved in 100 ml of absolute ethanol and 0.3 g of 10% Pd on carbon was added. Paar hydrogenation for 45 min, removal of the catalyst by filtration, and evaporation of the volatile material in vacuo yielded 1.54 g (91%) of crude **III**, which was utilized without purification in the next step. **III**, 1.54 g (0.0064 mol), and 0.73 g (0.0064 mol) of heptaldehyde were mixed together in an observably exothermic reaction and the product was dissolved in 100 ml of absolute ethanol. Paar hydrogenation for 1 h, removal of the catalyst by filtration and removal of the solvent in vacuo yielded

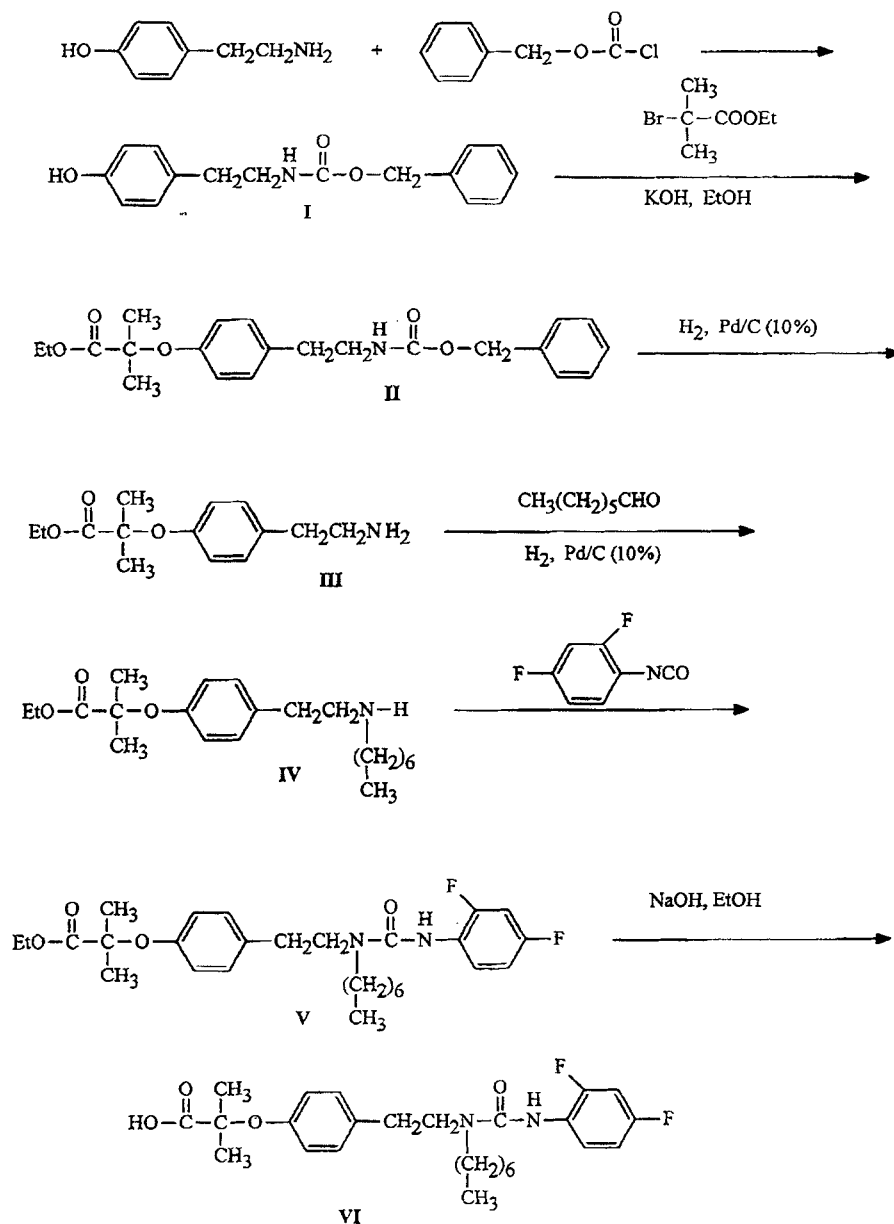


Fig. 2. Synthesis of 2-(4-(2-(N'-(2,4-difluorophenyl)-N-heptylureido)ethyl)phenoxy)-2-methylpropionic acid (compound 2).

2.13 g (95%) of crude IV as a colorless oil, which was utilized without purification in the next step. IV, 3.26 g (0.0093 mol) was dissolved in 100 ml of CH<sub>2</sub>Cl<sub>2</sub> and 1.55 g (0.01 mol) of 2,4-difluorophenylisocyanate was added. The resultant solution was stirred overnight, the solvent was removed in vacuo, and the residue was purified by flash chromatography (SiO<sub>2</sub>: 50 toluene/30 hexanes/10 CH<sub>2</sub>Cl<sub>2</sub>/ 10 EtOAc) to afford a nearly quantitative yield, 4.77 g, of V as a colorless oil. V, 2.4 g (0.0048 mol) was dissolved in 25 ml of absolute etha-

mol, and 100 ml of 1 N NaOH was added. The solution was stirred at room temperature for 4.5 h, 100 ml of 1 N HCl was added, and the aqueous solution was extracted with CH<sub>2</sub>Cl<sub>2</sub>. The organic layer was washed with H<sub>2</sub>O and a saturated aq. solution of NaCl, then dried over MgSO<sub>4</sub>. Filtration and removal of the solvent in vacuo yielded 2.46 g of a colorless oil, which was then purified by flash chromatography (SiO<sub>2</sub>: 1 hexanes/1 CH<sub>2</sub>Cl<sub>2</sub>/ 1 EtOAc) to yield 1.43 g (62%) of VI (compound 2) as a viscous, pale yellow oil.

## Animals

Male Sprague-Dawley (CD strain) rats (6–7 weeks of age) were obtained from Charles River Breeding Labs (Wilmington, MA). Rats were housed in wire mesh cages and maintained in an atmosphere of constant temperature ( $22 \pm 2^\circ\text{C}$ ) and relative humidity ( $55 \pm 5\%$ ) under a 12-h light cycle, 6 AM–6 PM, and allowed both food and water ad libitum.

To determine effects on serum cholesterol, rats (6/group) were fed standard rat chow containing 1% cholesterol and 0.5% cholic acid ad libitum for 3 days. During this time compounds to be tested for hypocholesterolemic activity were dissolved in 2.0 ml of 5% sodium bicarbonate solution and were administered by gavage once a day between 8:00 and 9:00 AM at doses of either 0.1, 1.0, or 10.0 mg/kg for the 3 days. Eighteen hours after the third dose, the rats were starved for 6 h and then bled via the abdominal vena cava while under anesthesia. Total serum cholesterol and HDL-cholesterol were determined enzymatically using Sigma diagnostic kits according to the prescribed procedures. Diet-induced increases in serum LDL + VLDL ranged from 183 to 227 mg/dl above the values for control chow-fed rats (73–91 mg/dl) in three experiments.

## Hepatocytes

Hepatocytes were isolated by collagenase (90 U/ml, 200 ml) perfusion for 9 min. Isolated cells were pelleted at 50 g and washed twice with collagenase-free RPMI 1640 medium containing 10% fetal bovine serum. Viability was determined by trypan blue exclusion, and was greater than 90%. Culture conditions were essentially as described by Lake et al. (26) except for the use of Vitrogen-coated plates and serum-free media. Briefly,  $1.5 \times 10^6$  hepatocytes were cultured on Vitrogen-coated plastic dishes in 2.0 ml of basal RPMI media supplemented with hydrocortisone (50  $\mu\text{g}/\text{ml}$ ), insulin (0.2 U/ml), and gentamicin (50  $\mu\text{g}/\text{ml}$ ). After a 4-h attachment period, media and nonviable cells were aspirated off and replaced with basal media to which various concentrations of bezafibrate or other test compound had been added in DMSO (0.4% final concentration). Media was changed at 24 h and after 48 h the media was aspirated and the cells were scraped into 4 ml saline and pelleted at 600 g. The hepatocyte pellets were then resuspended with sonication in 0.4 ml of 0.1 M  $\text{KPO}_4$  buffer, pH 7.4, and were subsequently assayed for laurate 12( $\omega$ )-hydroxylase activity. The combination of Vitrogen-coated plates and serum-free media resulted in greater bezafibrate induction of  $\omega$ -hydroxylase activity (20-fold) compared to the culturing of hepatocytes on plastic plates in 5% FCS-supplemented media.

## Enzyme preparation

Rats were killed by decapitation and the livers were quickly excised, trimmed, and chilled in ice-cold phosphate-buffered KCl (1.15% KCl in 0.25 M potassium phosphate, w/v, pH 7.4) homogenization buffer. All subsequent procedures were performed at 0–4°C. The livers were then blotted, weighed, and finely minced with scissors in 4 volumes of the ice-cold homogenization buffer. The 20% (w/v) liver homogenates were prepared using a Brinkman homogenizer (Model PT 10.35 equipped with a PTA 10S generator for <100 ml volumes) at a setting of 8 for 15–20 seconds. The homogenate was centrifuged at 10,000 g for 20 min and the resulting supernatant ( $S_{10}$ ) was subsequently used in the determination of in vivo hepatic laurate  $\omega$ -hydroxylase activity. Microsomes, used as the enzyme source for the ACAT assay, were obtained from the livers of rats that had been fed the 1% cholesterol and 0.5% cholic acid diet for 1 week and were prepared by a subsequent centrifugation of the  $S_{10}$  at 100,000 g for 1 h. Microsomal pellets were resuspended in 0.1 M  $\text{KPO}_4$  buffer, pH 7.4, to give a final suspension containing approximately 20–22 mg of microsomal protein per ml.

## Enzyme assays

Lauric acid 12-hydroxylase activity was routinely determined in 0.1 M  $\text{KPO}_4$  buffer, pH 7.4, containing 100  $\mu\text{M}$  [ $^{14}\text{C}$ ]lauric acid (5.0 mCi/mmol), 1.0 mM NADPH, and from 0.5 to 1.0 mg of whole cell homogenate, or 0.15–0.25 mg of  $S_{10}$  protein. Incubation volumes were 0.5 ml with whole cell homogenates or 1.0 ml with  $S_{10}$  protein. Whole cell homogenates were incubated at 37°C for 30 min and the incubations were terminated by the addition of 0.25 ml 4 N HCl. Incubations using  $S_{10}$  protein were terminated after 10 min with 0.5 ml 4 N HCl. Lauric acid and its hydroxylated products were extracted into 5 ml of ether. The organic layer was then removed and evaporated under  $\text{N}_2$ , and the extract was then resuspended in 200  $\mu\text{l}$  of the HPLC mobile phase used to separate the products of lauric acid metabolism. Lauric acid and its metabolites were analyzed by HPLC using a 10-micron silica column (Waters  $\mu\text{Porasil}$ ) and a mobile phase consisting of hexane–isopropanol–acetic acid 95:4:1 (v/v) at a flow rate of 1.0 ml/min for 20 min. All determinations were performed in duplicate and  $\omega$ -hydroxylase activity was calculated from the percent conversion of substrate as nanomoles of  $\omega$ -hydroxylauric acid formed per min per mg protein.

ACAT activity was assayed using [ $^{14}\text{C}$ ]oleoyl-CoA as the source for radiolabeling cholesterol ester (27). Microsomes (50–100  $\mu\text{g}$  protein), which had been pre-incubated at 37°C for 20 min at  $2\times$  concentrations of

DMSO or inhibitors added in DMSO (final concentration 0.4% DMSO), were then incubated in 0.2 ml of 0.1 M  $\text{KPO}_4$  buffer, pH 7.4, containing 5 nmol [ $^{14}\text{C}$ ]oleoyl-CoA (0.1  $\mu\text{Ci}$ ), 25  $\mu\text{M}$  bovine serum albumin, and 2 mM dithiothreitol. The reaction was terminated after 4 min at 37°C by extraction into 5.0 ml of ethanol–hexane 1:4(v/v). [ $^3\text{H}$ ]cholesterol (2.5  $\mu\text{g}$ ) and [ $^3\text{H}$ ]cholesterol oleate (2.5  $\mu\text{g}$ ) were added as internal standards. Recoveries were greater than 95% for both lipids. Dried hexane extracts were resuspended in 200  $\mu\text{l}$  of the HPLC mobile phase which consisted of acetonitrile–isopropanol–heptane 50:40:10(v/v/v) in 0.5% acetic acid. Chromatography was performed on a B&J OD5 Reverse Phase  $\text{C}_{18}$  column at a 1.0 ml/min flow rate. Column eluate was monitored with a Radiomatic FLO-OneBeta Radio-Chromatography detector. All assays were performed in duplicate and ACAT activity was calculated from the recovery of total pmoles of [ $^{14}\text{C}$ ]cholesteryl oleate formed per min per mg microsomal protein.

### Pharmacokinetic studies

In initial studies, hypocholesterolemic doses of **2** resulted in plasma concentrations in rats that were below the detection limit (50 ng/ml rat plasma) of our analytical method. To determine the optimal oral dose for studying the single dose pharmacokinetics of **2**, blood samples were obtained from groups of six rats 45 min after a single 2.0-ml oral dose of either 1, 10, 20, or 100 mg/kg of **2** in 5%  $\text{NaHCO}_3$  solution. From this study (see Study 1, Table 4) doses were selected for the intravenous and oral doses that were 50-fold and 200-fold greater than the hypocholesterolemic dose, respectively, so that the plasma concentrations of **2** remained within the range of quantitation over the period of the three half-life periods that the pharmacokinetics of **2** had established. Plasma concentrations and pharmacokinetics of **2** were determined in male rats after either a single 2.0-ml oral dose of 20 mg/kg in a 5%  $\text{NaHCO}_3$  solution or a 0.5-ml intravenous dose of 5 mg/kg in 5%  $\text{NaHCO}_3$  solution. At designated times after either the oral or intravenous dose, rats were anesthetized with  $\text{CO}_2$  and terminal blood samples were obtained from the vena cava. Groups of six rats were used at each of the following time points: 15, 30, 60 min, and 2, 4, 6, 8, 10, 12 h for the oral dose; and 5, 10, 15, 30, 60 min, and 2, 4, 8, 12 h for the intravenous dose. Plasma concentrations of **2** were determined by reversed phase HPLC. The analytical method utilized a  $\mu\text{Bondapak C}_{18}$  column (4.6  $\times$  30 cm) (Waters Inc., Milford, MA) and a mobile phase that consisted of 54% acetonitrile and 46% water containing 0.005 M octanesulfonic acid. The flow rate was 1 ml/min with the column heated to 55°C. Detection was by UV absorption at 200 nm. Sample preparation was done by solid phase extraction utilizing

a reversed phase  $\text{C}_{18}$  SepPak cartridge (Waters) and a QMA anion exchange SepPak cartridge.  $\text{C}_{18}$  cartridges were washed with 4 ml methanol followed by 6 ml water prior to use. A 0.5-ml plasma sample was loaded onto a  $\text{C}_{18}$  cartridge, washed with 2 ml water, and then eluted with 2 ml methanol. The methanol eluate was then introduced onto a QMA cartridge that had been pre-washed with 6 ml distilled water. After washing the methanol eluate with 4 ml distilled water, **2** was eluted with 2 ml of acidified water–methanol (50% 0.001 N HCl/50% methanol). A portion of the eluate could then be injected directly onto the HPLC. Quantitation was by external standardization and the linear range of detection was 50 ng/ml to 2000 ng/ml in rat plasma.

### Calculations and other procedures

Protein concentrations were determined using a Coomassie Blue reagent (28) with bovine serum albumin as standard.

The ACAT inhibitory potency was expressed as the micromolar concentration of a compound required to inhibit the enzyme activity by 50% ( $\text{IC}_{50}$ ).  $\text{IC}_{50}$ s for each compound were calculated from concentration–inhibition curves using at least six concentrations assayed in duplicate.

The intrinsic fibrate potency of a compound was defined as the concentration of a compound required to induce lauric acid  $\omega$ -hydroxylase activity to 50% (the  $\text{LA}_{50}$ ) of the maximal inducible level which is established with bezafibrate in each experiment. The  $\text{LA}_{50}$  for bezafibrate and for each compound tested was calculated from dose–response curves using at least six concentrations in duplicate plates. In order to control for the variability in the  $\text{LA}_{50}$ s which were observed between different hepatocyte preparations a Bezafibrate Index (B.I.) was calculated for each compound tested, where  $\text{B.I.} = \text{LA}_{50} \text{ for bezafibrate} / \text{LA}_{50} \text{ for tested compound}$ . This normalization allowed for the comparison of intrinsic fibrate potencies for different compounds that were synthesized and tested over a 4-year period.

Plasma concentration–time data of **2** were analyzed using noncompartmental pharmacokinetic methods and Microsoft Excel.  $C_{\text{max}}$  and  $t_{\text{max}}$  were obtained from direct inspection of the plasma concentration–time data. The  $t_{1/2}$  was calculated as  $\ln(2)/k_{\text{el}}$ , where  $k_{\text{el}}$  is the first-order elimination rate constant determined by the slope of the linear regression line of the apparent terminal linear portion of the log concentration versus time curve.  $\text{AUC}_{0 \rightarrow t}$  was calculated using the linear trapezoidal method from zero to time  $t$ , where  $t$  is the last time point with a measurable concentration of **2**.

Statistical differences were determined by Student's  $t$  test and the level of significance was set at  $P < 0.05$ .

## RESULTS

Figure 1 depicts the structures and ACAT inhibitory potencies for LR-16, the prototypical ureidophenoxyisobutyrate (29), and for CL277,082, Lederle's urea-based ACAT inhibitor (16, 30). Also depicted in Fig. 1 are two related analogues which attempt to incorporate the salient structural features of LR-16 and CL277,082. These two related analogues were used to investigate the structural basis for the 100-fold difference in ACAT inhibitory potency between LR-16 and CL277,082. While the two analogues (BW-USC-209 and BW-USC-148) maintain the trisubstituted urea nucleus of CL277,082 by incorporating an N-heptyl alkyl chain (Y) and a substituted benzyl moiety (Z), they differ from CL277,082 by the replacement of the neopentylbenzyl group with a phenoxyisobutyrate group that is a characteristic of most fibrates including LR-16. As a consequence of maintaining the trisubstituted urea nucleus of CL277,082, these two fibric acid derivatives possessed approximately 5-fold greater ACAT inhibitory potency than LR-16. Because different halogen substitutions on the ureidophenyl ring for BW-USC-209 and BW-USC-148 resulted in only slight differences in their ACAT  $IC_{50}$ s, it can be concluded that the presence of the phenoxyisobutyrate moiety is largely responsible for the lower ACAT inhibitory potency in these and in other similar fibric acid derivatives compared to the neopentyl substitution on the ureido benzyl group as in CL277,082.

To assess the intrinsic fibrate activity of LR-16 and the two phenoxyisobutyrate derivatives of CL277,082, the compounds were tested for their ability to induce the level of laurate  $\omega$ -hydroxylase activity in primary cultures of rat hepatocytes. As stated in Methods, the intrinsic fibrate potency (or  $LA_{50}$ ) of a compound was defined as the concentration of a compound required to induce laurate  $\omega$ -hydroxylase activity in rat hepatocyte cultures to 50% of the maximal induced level that was established with bezafibrate in every experiment. **Figure 3A** depicts bezafibrate dose-response curves from five different hepatocyte cultures covering a recent 12-month period. As seen in this figure, the maximal induced level of laurate  $\omega$ -hydroxylase activity varied by almost 2-fold (compare MF9443 vs. MF9430) although the  $LA_{50}$ s for bezafibrate were comparable. In other experiments (data not shown), the  $LA_{50}$  for bezafibrate ranged as high as 10  $\mu$ M compared to the average value of  $5.2 \pm 0.8 \mu$ M for the five experiments illustrated in Fig. 3A. Although standardized hepatocyte isolation procedures and culture conditions were used throughout the 4-year period in which these compounds were synthesized and tested, the 2.5-fold range for the bezafibrate  $LA_{50}$  suggests that subtle differences in hepato-

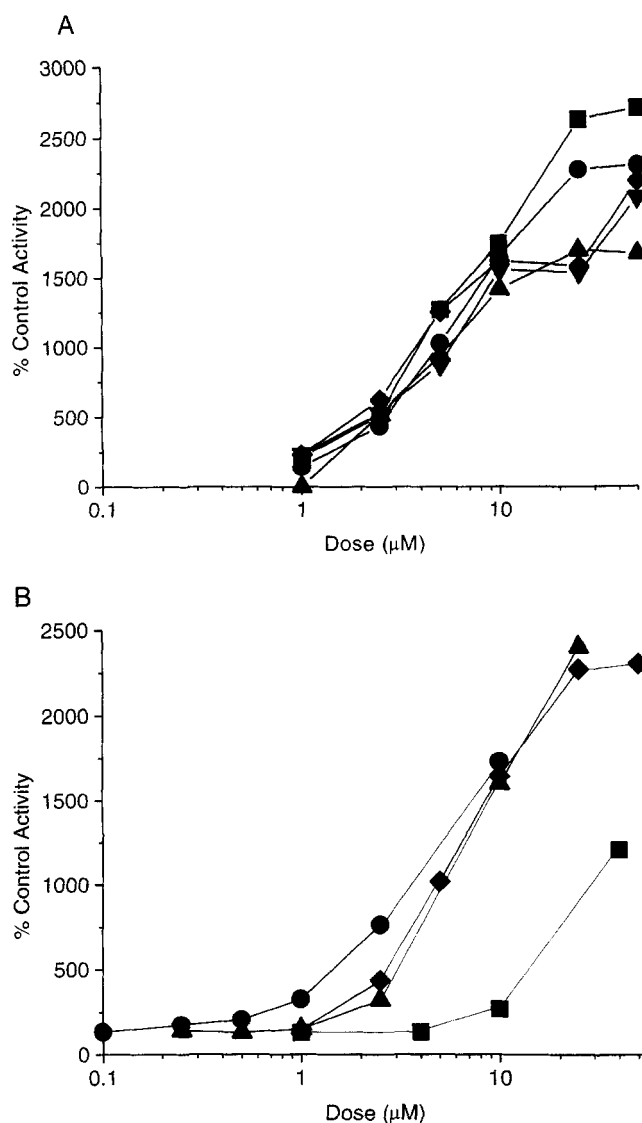


**Fig. 3.** Induction of lauric acid 12-hydroxylase activity in primary cultures of rat hepatocytes by bezafibrate, LR-16, BW-USC-209, and BW-USC-148. A: dose-response curves for bezafibrate using five different hepatocyte preparations. Symbols and the  $LA_{50}$  values for each of the five experiments are as follows: MF9430, ■, 6.1  $\mu$ M; MF9436, ●, 5.7  $\mu$ M; MF9443, ▲, 4.2  $\mu$ M; MF9449, ▼, 5.4  $\mu$ M; and MF9364, ◇, 4.5  $\mu$ M. B: The symbols and  $LA_{50}$  values for each of the compounds depicted are as follows: bezafibrate, ■, 5.9  $\mu$ M; BW-USC-148, ◇, 6.2  $\mu$ M; BW-USC-209, ●, 4.4  $\mu$ M; and LR-16, ▲, 30.1  $\mu$ M.

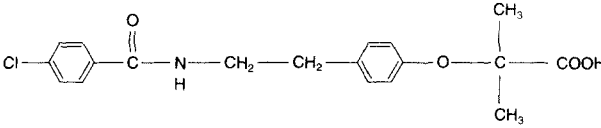
cyte preparations can affect the determination of an  $LA_{50}$ . Differences in cell membrane permeability or in cell viability as a result of the collagenase digestion procedures used in hepatocyte isolation could invariably affect the responsiveness of the hepatocytes to drug treatment and the level of enzyme induction attained. Therefore, to control for possible variability in the determination of a compound's intrinsic fibrate potency, the  $LA_{50}$  for a given compound was normalized to the

LA<sub>50</sub> for bezafibrate (bezafibrate LA<sub>50</sub>/compound LA<sub>50</sub>). This bezafibrate index (B.I.) allowed for the comparison of potencies of compounds tested in different hepatocyte preparations.

The dose-response curves describing the intrinsic fibrate potencies for bezafibrate and for LR-16 and the two CL277,082 analogues are depicted in Fig. 3B. While the compounds were tested at six concentrations ranging from 1  $\mu$ M to 250  $\mu$ M, not all concentrations could be used for LA<sub>50</sub> determination. Cell toxicity was suspected at higher drug concentrations when the drug failed to achieve the maximal level of enzyme activity or when there was a significant loss of enzyme activity with increasing dose. Although the data at the higher concentrations are not depicted in Fig. 3B for clarity of graphic presentation, BW-USC-209 was found to be the least tolerated compound, causing activity to decrease by 63% at 40  $\mu$ M from the maximally induced level which was attained at 10  $\mu$ M. BW-USC-209 (B.I. = 1.4) was found to be slightly more potent than either bezafibrate (B.I. = 1.0) or BW-USC-148 (B.I. = 1.0), while LR-16 was significantly less potent than bezafibrate (B.I. = 0.2). Therefore, an approximately 7-fold increase in intrinsic fibrate potency (compare LR-16 vs. BW-USC-209) was obtained by incorporating an N-heptyl alkyl chain and a substituted ureidobenzyl group which are important structural features for the potent ACAT inhibitory activity in Lederle's CL277,082 (31). These results indicated that novel trisubstituted ureidophenoxyisobutyrate analogues could possess greater ACAT inhibitory activity and still maintain a similar intrinsic fibrate potency when compared to some currently used potent fibric acid derivatives. These results provided the basis for examining in greater detail the effect of additional methylene substitution in the urea bridging region between the two aromatic rings (see Table 2), and the effects of N-alkyl substitution (see Table 3) within this difluoro, trisubstituted, ureidophenoxyisobutyrate series.

**Table 1** depicts the normalized intrinsic fibrate potency (the bezafibrate index) and ACAT inhibitory activity for clofibrate and for several clofibrate analogues which are often referred to as the "second-generation" fibrates (see Table 5). As seen in this table, these second-generation fibrates are characterized by an approximately 20-fold greater intrinsic fibrate potency and significantly greater ACAT inhibitory potency compared to clofibrate. These enhanced activities may partly explain the better pharmacological profiles which have been observed clinically with the second-generation derivatives. Also depicted in Table 1 is the effect of substitution of the nitrogen atom in bezafibrate with alkyl chains of increasing length to determine whether an analogous nitrogen trisubstitution in a different fibrate

TABLE 1. Intrinsic fibrate potency and ACAT inhibitory activity of bezafibrate and N-alkyl analogues of bezafibrate, clofibrate, and other clofibrate derivatives

Structure of bezafibrate	Bezafibrate Index	ACAT Inhibitory Activity IC <sub>50</sub>
		$\mu$ M
		
Bezafibrate	1.0	144
N-Methyl bezafibrate	0.7	285
N-Butyl bezafibrate	2.7	29.4
N-Heptyl bezafibrate	2.4	8.4
N-Decyl bezafibrate	N.E. <sup>a</sup>	8.1
Clofibrate	0.1	N.E. <sup>b</sup>
Fenofibric acid	2.7	107
Ciprofibrate	1.7	143
Beclibrate	1.4	55

<sup>a</sup>No effect on laurate 12-hydroxylase activity from 1  $\mu$ M to 250  $\mu$ M in cultures of rat hepatocytes.

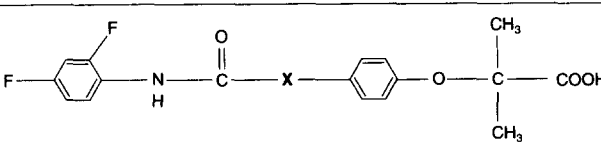
<sup>b</sup>No effect on hepatic microsomal ACAT activity from 100  $\mu$ M to 1 mM.

derivative might result in similar enhancements in ACAT inhibitory potency as was observed with the ureido compounds depicted in Fig. 2. An approximately 35-fold increase in ACAT inhibitory potency was obtained by lengthening the alkyl substitution of the amide nitrogen from C<sub>1</sub> to C<sub>7</sub>. Perhaps more importantly, substitution of the amide nitrogen with alkyl chains of C<sub>4</sub> and C<sub>7</sub> also increased the intrinsic fibrate potency for bezafibrate by 2.5-fold. This latter result was analogous to the effect that trisubstitution had on intrinsic fibrate potency with the urea analogues which were studied initially (see Fig. 3B). The lack of any further enhancement of activities with the C<sub>10</sub> analogue may have been due to the insolubility encountered with this compound in the assays.

**Table 2** and **Table 3** depict experiments that examined in greater detail the effect of substitution of the ureido monomethylene region in the ureido fibrate analogues studied initially, on intrinsic fibrate potency. The impact of these structural modifications on the ability of these analogues to lower serum VLDL + LDL cholesterol in a hypercholesterolemic rat model was also studied in these experiments to determine the pharmacological importance of this chemical series. In Table 2, **X** represents the urea nitrogen substituted with R, which is a C<sub>7</sub> alkyl chain and is not varied, and with a monomethylene linkage to the phenoxyisobutyrate acid moiety as in the case of **1**. Compound **1**, the free acid of BW-USC-148, possessed an intrinsic fibrate potency similar to the original ethyl ester which suggested



TABLE 2. Intrinsic fibrate potency of various heptyl substituted phenoxyisobutrates



Compound	X (where R = heptyl)	Bezafibrate Index	Hypocholesterolemic Activity
Dose for 40–50% lowering			
1	–NRCH <sub>2</sub> –	0.7	>10 mg/kg
2	–NR(CH <sub>2</sub> ) <sub>2</sub> –	167.0	0.1 mg/kg
3	–NR(CH <sub>2</sub> ) <sub>3</sub> –	25.2	1.0 mg/kg
4	–CHR(CH <sub>2</sub> ) <sub>2</sub> –	27.4	1.0 mg/kg
5	–NRCH <sub>2</sub> CHOH–	5.0	N.E. <sup>a</sup>

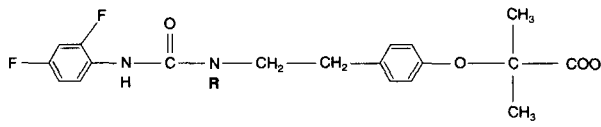
<sup>a</sup>No effect on serum VLDL + LDL cholesterol at 10 mg/kg per day, p.o.

that cultures of primary rat hepatocytes efficiently de-esterify the simple prodrug ester forms of clinically used fibrates. At 10 mg/kg per day, which was the highest dose tested in hypercholesterolemic rats, **1** decreased serum LDL + VLDL cholesterol by only 24%. When the number of carbon atoms in the methylene linkage between the urea nitrogen and the phenoxyisobutyrate group was increased to two (i.e., **2**), an unexpected 200-fold increase in the intrinsic fibrate potency was obtained. Compound **2** routinely induced laurate  $\omega$ -hydroxylase activity in rat hepatocyte cultures over a concentration range of 5–100 nM with an LA<sub>50</sub> of 36 ± 15 nM (mean ± SD for three experiments, data not shown), compared to an LA<sub>50</sub> of 1–20 μM for bezafibrate (refer to Fig. 3). The extraordinarily high B.I. (167 ± 40, n = 3) for this analogue was approximately two orders of magnitude greater than the B.I.s for the most potent, currently used fibrates (see Table 1). The hypocholesterolemic activity of **2** was evaluated to determine the significance of this high index. In hypercholesterolemic rats, **2** decreased diet-induced serum LDL + VLDL cholesterol by 40–50% at a dose of 0.1 mg/kg per day in three separate experiments and was ~500-fold more potent than some second-generation fibrate standards which were also tested. The complete hypocholesterolemic dose–response curves for **2** and for three fibrate standards are depicted in Fig. 4A. For greatest intrinsic fibrate activity, the optimal configuration of the bridging region between the two aromatic rings appeared to be comprised of a C<sub>7</sub> substituted urea moiety linked by a dimethylene to the phenoxyisobutyrate group as in **2**. When a third methylene carbon was incorporated into the urea linkage (i.e., **3**) or when the trisubstituted nitrogen atom was replaced by a carbon atom (i.e., **4**) then intrinsic fibrate potency decreased

by ~6-fold and hypocholesterolemic activity decreased by 10-fold. Within the bridging region in **2**, there is a structural feature that is shared with bezafibrate. This consists of the substituted nitrogen atom linked by a dimethylene to the phenoxyisobutyrate group. The effect of potential metabolism in this bridging region on the intrinsic fibrate activity of **2** was examined with the hydroxylated analogue **5**, as a similar benzylic hydroxylated metabolite had been reported for bezafibrate in humans (32). The presence of a benzylic hydroxyl group resulted in a greater than 30-fold decrease in the intrinsic fibrate potency for this compound and a complete loss of hypocholesterolemic activity at the 10 mg/kg per day dose. These results further defined the optimal configuration of the bridging region between the two aromatic rings containing the trisubstituted urea nitrogen.

Structural requirements for **R**, the C<sub>7</sub> alkyl chain substituent of the trisubstituted nitrogen moiety in earlier analogues, were then examined in the experiments depicted in Table 3. In the absence of an N-alkyl chain substitution (**6**) the intrinsic fibrate potency (B.I. = 1.0) was much lower than that was observed with the C<sub>7</sub> N-alkyl analogues even though **6** possessed the optimal configuration for the bridging region between the aromatic rings as in **2** (B.I. = 167). Similar to bezafibrate (see Fig. 4A), **6** had no effects on serum VLDL + LDL cholesterol at a dose of 10 mg/kg per day. The C<sub>7</sub> N-alkyl chain substituent was found to be optimal for greatest intrinsic fibrate potency and hypocholesterolemic activity when the N-alkyl chain length was selectively varied from C<sub>5</sub> to C<sub>11</sub>. The effects of cyclization or

TABLE 3. Intrinsic fibrate potency of N-alkylureido phenoxyisobutrates



Compound	R	Bezafibrate Index	Hypocholesterolemic Activity
Dose for 40–50% lowering			
6	H	1.0	N.E. <sup>a</sup>
7	–(CH <sub>2</sub> ) <sub>4</sub> CH <sub>3</sub>	57.5	1.0 mg/kg
2	–(CH <sub>2</sub> ) <sub>6</sub> CH <sub>3</sub>	167.0	0.1 mg/kg
8	–(CH <sub>2</sub> ) <sub>8</sub> CH <sub>3</sub>	4.6	10 mg/kg
9	–(CH <sub>2</sub> ) <sub>10</sub> CH <sub>3</sub>	2.2	N.D. <sup>b</sup>
10	–(CH <sub>2</sub> ) <sub>6</sub> COOH	<0.1 <sup>c</sup>	N.E.
11	–cycloheptyl	5.1	>10 mg/kg
12	–(CH <sub>2</sub> )–cycloheptyl	28.5	1.0 mg/kg

<sup>a</sup>No effect on serum LDL + VLDL cholesterol at 10 mg/kg per day, p.o.

<sup>b</sup>Not determined.

<sup>c</sup>No effects on laurate 12-hydroxylase activity from 1 μM to 250 μM in cultures of rat hepatocytes.

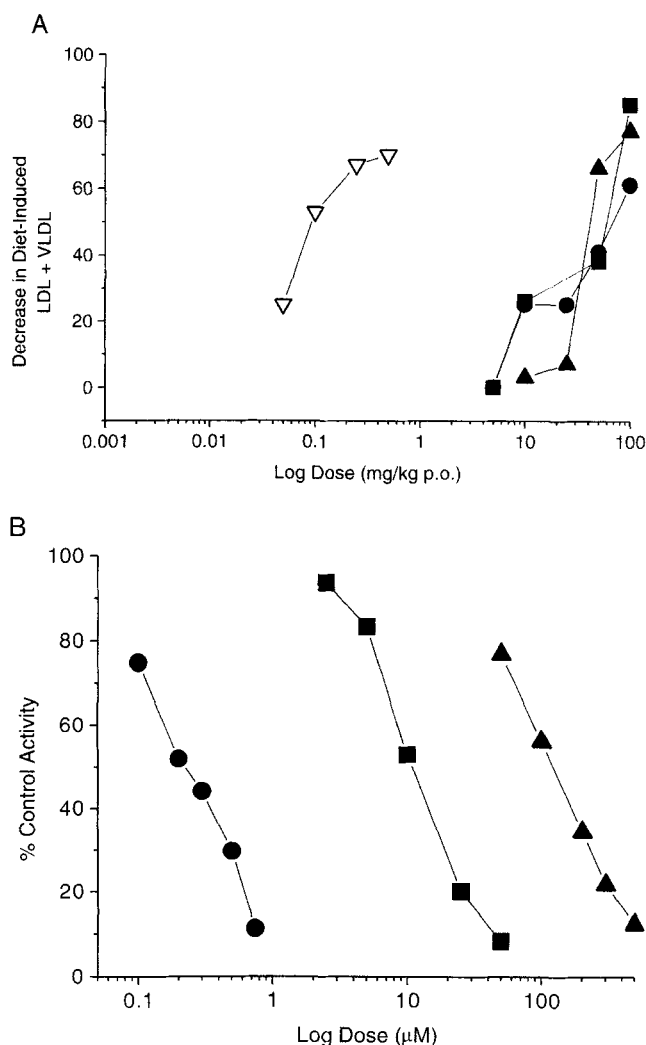


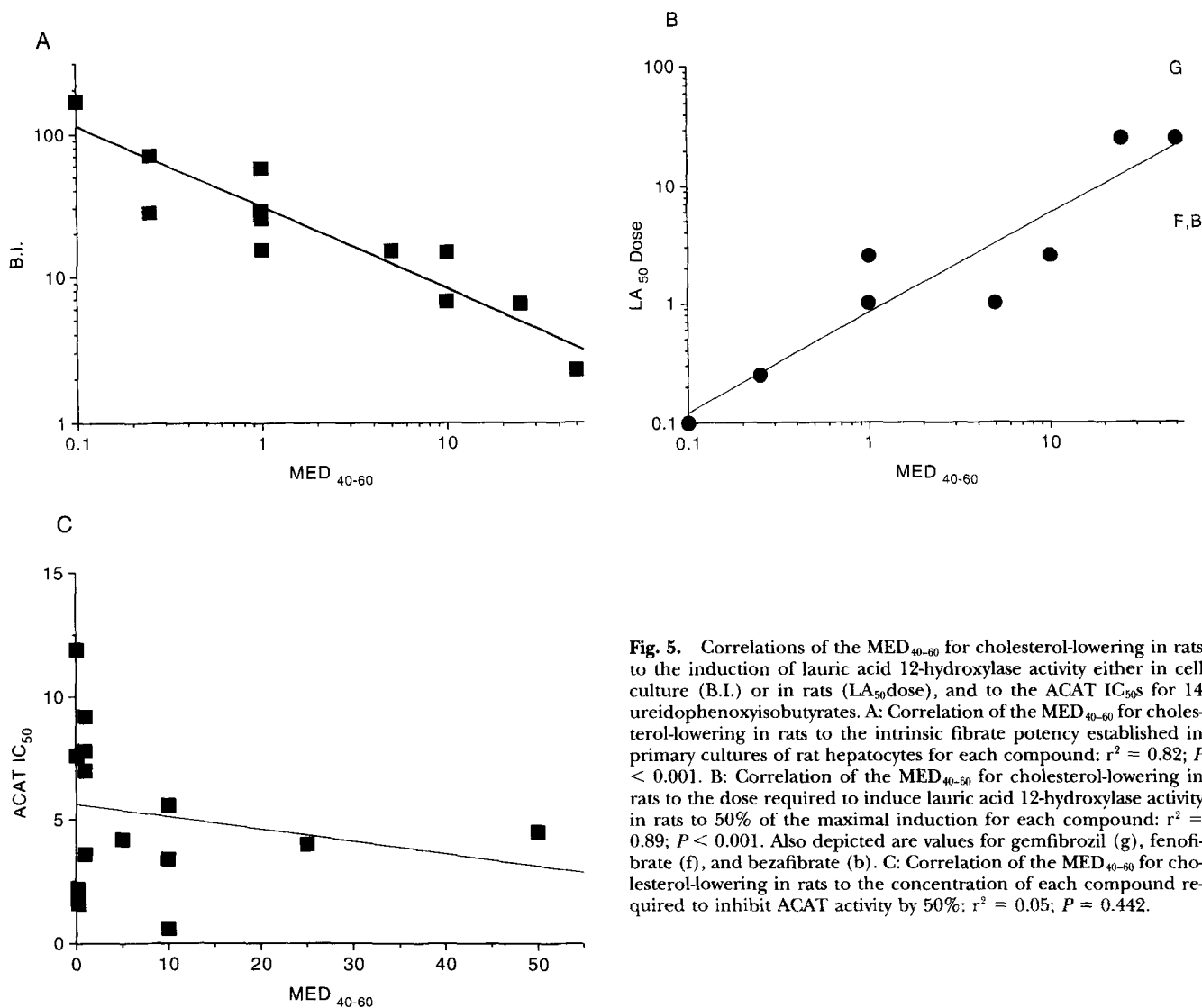
**Fig. 4.** In vivo hypocholesterolemic activity and in vitro ACAT inhibitory activity of **2** and other fibrates. **A:** The effects of **2** versus gemfibrozil, bezafibrate, and fenofibrate on serum VLDL + LDL cholesterol in cholesterol-fed rats. Data are depicted as the percent decrease from the diet-induced concentrations of VLDL + LDL in vehicle treated control rats at each dose. The symbols for each compound are as follows: **2**, V; bezafibrate, ■; fenofibrate, ●; and gemfibrozil, ▲. **B:** The dose-response effects of **2** versus bezafibrate and CL277,082 on ACAT activity assayed using hepatic microsomes prepared from cholesterol-fed rats. The symbols and  $IC_{50}$  concentrations for each compound are as follows: CL277,082, ●, 0.24  $\mu$ M; **2**, ■, 11.5  $\mu$ M; and bezafibrate, ▲, 120  $\mu$ M.

oxidation of the  $C_7$  alkyl chain on the bezafibrate index were also examined as straight N-alkyl chains in other ureido and amido ACAT inhibitors have been shown to be susceptible to  $\omega$ -oxidation followed by  $\beta$ -oxidation (33, 34). As seen in Table 3, replacement of the  $C_7$ N-alkyl chain with an N-cycloheptyl group (**11**) resulted in a significant decrease in both intrinsic fibrate potency and hypocholesterolemic activity (25% decrease in LDL + VLDL cholesterol at 10 mg/kg per day). In contrast, substitution of an N-cycloheptylmethyl group

(**12**) for the  $C_7$ N-alkyl chain resulted in an approximately 6-fold greater intrinsic potency and hypocholesterolemic activity compared to the N-cycloheptyl analogue. The addition of the methylene between the cycloheptyl group and the trisubstituted urea nitrogen may have imparted more flexibility in this area of the molecule allowing the N-alkyl substituent to assume a conformation more similar to the straight  $C_7$ N-alkyl chain and, therefore, achieve greater intrinsic fibrate activity. Similar to the results obtained with the benzylic hydroxyl analogue (i.e., **5**), incorporation of a terminal carboxyl group on the  $C_7$ N-alkyl chain (**10**) resulted in a complete loss of intrinsic fibrate potency and hypocholesterolemic activity. These results suggest that the most likely pathways of phase I metabolism in the region of the trisubstituted urea nitrogen, which would include benzylic hydroxylation and/or  $\omega$ -hydroxylation/ $\beta$ -oxidation, will result in a significant loss in the pharmacological activity of these novel hypolipidemic agents. These results also suggest that lipophilicity in the area of the trisubstituted nitrogen must be important for interaction with the receptor site or other mechanism by which these compounds exert their pharmacological effects.

Throughout the evaluation of these compounds, the B.I. for a given compound appeared to be a good predictor of its relative hypocholesterolemic potency compared to bezafibrate. For example, **2** had the greatest intrinsic fibrate activity (B.I. = 167) and an  $ED_{50}$  of 0.1 mg/kg per day for hypocholesterolemic activity which was the lowest among the 12 ureido compounds tested, and was 500-fold more potent than any of the second generation fibrates tested in hypercholesterolemic rats (see Fig. 4A). In contrast, the potent hypocholesterolemic activity of these compounds could be the result of greater inhibitory effects on hepatic ACAT activity when compared to other fibrates. Figure 4B compares the dose-response effects of **2** to the effects of CL277,082 and bezafibrate on rat hepatic microsomal ACAT activity. Consistent with results obtained with the previous CL277,082 ureido fibrate analogues, **2** was found to inhibit ACAT activity with an approximately 10-fold greater potency than bezafibrate.

To examine whether the increased hypocholesterolemic potency of these novel ureido derivatives resulted from either their greater intrinsic fibrate activity or from their enhanced ACAT inhibitory activity, the minimal effective dose resulting in a 40–60% hypocholesterolemic effect in rats (the  $MED_{40-60}$ ) was plotted against either the ACAT inhibitory potency (the ACAT  $IC_{50}$ ) or the intrinsic fibrate potency (the B.I.) for 14 structurally similar ureido fibrate analogues. These correlations are presented in Fig. 5 along with a correlation of the  $MED_{40-60}$  to the oral dose (mg/kg per day) re-



quired to induce hepatic lauric acid  $\omega$ -hydroxylase activity to 50% of the maximal inducible level (the LA<sub>50</sub> dose) that was also determined for each analogue in hypercholesterolemic rats. As seen in Fig. 5, the MED<sub>40-60</sub> was highly correlated over a 100-fold range to the B.I. ( $r^2 = 0.82$ , see Fig. 5A) but not to the ACAT IC<sub>50</sub> which only varied over a 10-fold range ( $r^2 = 0.05$ , see Fig. 5C). These results suggest that the enhanced ACAT inhibitory activity of these novel trisubstituted ureido fibrate derivatives does not contribute significantly to their greater hypocholesterolemic activity. Potential effects on intestinal ACAT activity should be minimized because drug and dietary cholesterol were administered approximately 12 h apart. Importantly, the LA<sub>50</sub> dose was also highly correlated to the MED<sub>40-60</sub> ( $r^2 = 0.89$ , see Fig. 5B) and therefore to the B.I.. This latter result indicates that these compounds share similar and favorable pharmaco-

**Fig. 5.** Correlations of the MED<sub>40-60</sub> for cholesterol-lowering in rats to the induction of lauric acid 12-hydroxylase activity either in cell culture (B.I.) or in rats (LA<sub>50</sub>dose), and to the ACAT IC<sub>50</sub>s for 14 ureidophenoxyisobutyrate derivatives. A: Correlation of the MED<sub>40-60</sub> for cholesterol-lowering in rats to the intrinsic fibrate potency established in primary cultures of rat hepatocytes for each compound:  $r^2 = 0.82$ ;  $P < 0.001$ . B: Correlation of the MED<sub>40-60</sub> for cholesterol-lowering in rats to the dose required to induce lauric acid 12-hydroxylase activity in rats to 50% of the maximal induction for each compound:  $r^2 = 0.89$ ;  $P < 0.001$ . Also depicted are values for gemfibrozil (g), fenofibrate (f), and bezafibrate (b). C: Correlation of the MED<sub>40-60</sub> for cholesterol-lowering in rats to the concentration of each compound required to inhibit ACAT activity by 50%:  $r^2 = 0.05$ ;  $P = 0.442$ .

kinetic characteristics in the rat as the estimation of their intrinsic fibrate activities or their abilities to induce hepatic lauric acid  $\omega$ -hydroxylase activity could be obtained in either rat hepatocyte cultures or in vivo and could be correlated with an in vivo pharmacological response. The correlation of either the B.I. or the LA<sub>50</sub> dose to the MED<sub>40-60</sub> would seem to indicate a causal relationship between enzyme induction and cholesterol-lowering activity. However, this was only true for the ureido fibrate analogues. As seen in Fig. 5B, the ratio of the MED<sub>40-60</sub> to the LA<sub>50</sub> dose was 10:1 for bezafibrate and fenofibrate but 1:2 for gemfibrozil, compared to ratios near 1:1 for several trisubstituted ureido fibrate analogues. Other investigators have reported the lack of correlation between enzyme induction and the hypolipidemic response of fibrates (35–38).

The single-dose pharmacokinetics of **2** was studied in

TABLE 4. Determination of single-dose pharmacokinetics of compound **2** in the rat

Study 1: 0.75 h Post-Dose Plasma Levels of <b>2</b>		
Oral Dose	Plasma Concentration*	
mg/kg	µg/ml	
1	0.13 ± 0.04	
10	7.10 ± 0.50	
20	14.38 ± 2.00	
100	21.65 ± 1.64	
Single Dose Pharmacokinetics for <b>2</b> in the Rat		
Variable	5 mg/kg I.V.	20 mg/kg P.O.
$t_{1/2}$	3.0 h	—
AUC	12.5 µg · h/ml	37.4 µg · h/ml
$C_{max}$	—	15.41 ± 2.20 µg/ml
$t_{max}$	—	0.5 h

\*A  $1/c^2$  weighted linear regression model was used to calculate the plasma concentrations from peak areas obtained using a VG ChromServer and Multichrom software (version 1.8-3, Fisons Instruments, Altricham, UK).

rats to establish a relationship between the hypocholesterolemic potency of the trisubstituted ureido fibrate analogues and plasma concentration. As discussed in Methods, the optimal oral dose for studying the single dose pharmacokinetics of **2** was selected by first determining the plasma concentrations of **2** at 45 min (the approximate  $t_{max}$ ) after oral doses between 1 mg/kg and 100 mg/kg. As seen in Table 4 (see Study 1), **2** appeared to be well absorbed over the dose range studied with 1 mg/kg being the lowest dose for which our analytical method had adequate sensitivity to detect peak plasma but not serial plasma concentrations. Between 1 mg/kg and 10 mg/kg the approximate  $C_{max}$  plasma concentration of **2** increased approximately 50-fold. In contrast, the plasma concentration increased 2-fold between 10 mg/kg and 20 mg/kg. The 20 mg/kg dose was selected for the pharmacokinetic study in order to follow decreases in plasma concentrations of **2** over a period of at least three half-life periods. These data suggest that at the hypolipidemic dose or the  $MED_{40-60}$  for **2**, which is a 200-fold lower dose than what could be studied, the  $C_{max}$  can be expected to be well below the 50 ng/ml limit of detection of our method and drug exposure will be very low compared to the other fibrates (see below). As seen in Table 4, the 20 mg/kg oral dose of **2** was rapidly ( $t_{max} = 0.5$  h) and extensively ( $F = 0.75$ ) absorbed with a  $C_{max}$  of  $15.41 \pm 2.20$  µg/ml. The elimination half-life was 3 h and total exposure as estimated by AUC was  $37.4$  µg · h/ml. In contrast, 100-fold greater AUCs have been reported for other fibrates at their hypocholesterolemic doses in rats. Ciprofibrate has been reported to have an elimination half-life of 48 h and an AUC of  $4900$  µg · h/ml and a  $C_{max}$  of  $57$  µg/ml after a single oral dose of 10 mg/

kg (39). In contrast, bezafibrate was reported to have an elimination half-life of 4 h in rats, and an AUC of  $2100$  µg · h/ml and a  $C_{max}$  of  $167$  µg/ml after an oral dose of 125 mg/kg (39). Ciprofibrate has an intrinsic fibrate activity similar to bezafibrate (see Table 1) but effects on serum lipids are observed at 10-fold lower doses in rats because of its slower rate of clearance. These data indicate that it is the 100-fold increase in the intrinsic potency of **2** that results in cholesterol-lowering doses and AUCs for **2** that are at least 100-fold lower compared to other fibrates. Therefore, total drug exposure (the AUC) will be significantly less with **2** during chronic treatment of rats at hypolipidemic doses and may result in a better therapeutic ratio for this compound even when compared with bezafibrate which has a similar elimination half-life.

## DISCUSSION

We show here that the potent hypocholesterolemic activity of a novel series of ureidophenoxyisobutyrate results from an enhanced intrinsic property of these molecules due to the presence of a lipophilic nucleus containing a trisubstituted nitrogen optimally substituted with a  $C_7$  alkyl chain. This intrinsic activity may be the result of some highly specific interaction of these compounds with a protein or receptor involved in their mechanism(s) of action. The induction of several peroxisomal enzymes by fibrates and other peroxisomal proliferators has now been shown to be due to the activation of a family of nuclear hormone receptors termed peroxisome proliferator-activated receptors (PPARs) (for reviews see 40, 41). Recently, the direct binding of 15-deoxy-prostaglandin  $PGJ_2$  (15-d- $PGJ_2$ ) and BRL49653 of the thiazolidinedione family of insulin sensitizers to the PPAR $\gamma$  subtype has been described (42–45). This suggests that the activation of other PPARs by peroxisomal proliferators may be mediated through similar ligand–receptor interactions. Although no direct receptor binding to any of the PPARs has been observed with the classical fibrates to date, the intrinsic binding activity of these agents may be too low to allow detection of receptor binding. It has been reported that PPAR $\alpha$  binds specifically as a heterodimer with the retinoid X receptor to a peroxisome proliferator response element (PPRE) identified in the CYP4A1 promoter (46–48). CYP4A1 is a rat liver microsomal cytochrome P450 isozyme that is involved in the  $\omega$ -hydroxylation of fatty acids and prostaglandins, and in the metabolism of xenobiotics (23, 49). The correlation in rats of hypocholesterolemic activity with induction of hepatic lauric acid  $\omega$ -hydroxylase activity either in culture or in vivo

TABLE 5. Literature values for the steady-state plasma concentrations of various fibrates at hypocholesterolemic doses in humans

Fibrate	Daily Human Dose	Elimination $t_{1/2}$	Plasma Concentrations at Steady State	Reference
	mg/day		$\mu\text{g/ml}$	
Clofibrate	1500–2000	15–22	125–162	56
Second generation fibrates				
Bezafibrate	600	2.1	3–4	57
Fenofibrate	100–300	20–26	10	56
Beclobrate	100–200	15–18	2	58
Ciprofibrate	100	42–72	30 <sup>a</sup>	59

<sup>a</sup>Personal communication from Dr. Bruce Berger at Winthrop-Sterling.

suggests that PRAR $\alpha$  may be involved in the activation of the gene(s) responsible for the cholesterol-lowering activity. As discussed above, such a correlation has not been reported with other fibrates in rats, suggesting that these ureido fibrates may have greater specificity in their target gene activation. Indeed, we have found that the increased hypocholesterolemic potency of the trisubstituted ureido fibrate analogues described here correlates with both their greater induction of PPAR $\alpha$  activity in a transient transfection assay and their high affinity binding to the receptor (unpublished results). Although the activation of genes in the CYP4 family (50) as well as genes associated with peroxisomal proliferation is characteristic of fibrate action in rodents, these pleiotypic responses are not elicited in humans. It may be that analogous human genes such as P450HL $\omega$ , which is a human hepatic fatty acid  $\omega$ -hydroxylase that has recently been identified as a member of the CYP4A subfamily (51), lack the specific PPREs which results in gene activation by fibrates. In contrast, other genes that mediate effects of fibrates on lipoprotein metabolism may be similarly regulated in rats and humans such as in the suppression of the rat and human apoC-III gene by fenofibrate (52–54).

Importantly, the greater hypocholesterolemic potency of these ureido fibrate analogues is not a result of their greater ACAT inhibitory activity, which is also attributed to the presence of the lipophilic trisubstituted nitrogen. In addition, the lower pharmacological doses that are required as a result of the more than 100-fold increase in the intrinsic activity of these compounds may result in a better safety profile compared to other agents in this class due to lower total drug exposure especially to peripheral tissues. The similar side-effect profile, which characterizes the “second-generation” fibrates (55) and which has limited their clinical usefulness, may result from the similar steady-state plasma concentrations that are achieved during therapy. When compared to clofibrate in humans, the “second-generation” fibrates are characterized by lower

steady-state plasma concentrations and lower doses (see Table 5 literature values) presumably because of their greater intrinsic fibrate activity. Similar to what is observed in rats, differences in the daily human dose between second-generation fibrates may result more from differences in their clearances (compare bezafibrate to ciprofibrate in Table 5) than to differences in their intrinsic properties. In contrast, the novel trisubstituted ureido fibrate derivatives may demonstrate an improved safety profile, even in the rat, because of target gene specificity and decreased drug exposure by virtue of the increased intrinsic activities which these compounds possess. ■

The authors wish to thank Laurene Wang for the pharmacokinetic analysis of the plasma concentration-time data; Mark Player, Zhendong Wu, Kazimierz Seyda, and Muhdi Sadikan for the synthesis of the described compounds; and Scott Sundseth and Melissa Foshee for their help with the animal and cell culture experiments. We also wish to thank Dr. Thomas Krenitsky, former Vice-President of Research, Burroughs Wellcome Co., who supported and encouraged the development of this project.

Manuscript received 11 November 1996, in revised form 2 February 1997, and in re-revised form 14 March 1997.

## REFERENCES

- Illingworth, D. R., and J. A. Tobert. 1994. A review of clinical trials comparing HMG-CoA reductase inhibitors. *Clin. Ther.* **16**: 366–385.
- Sirtori, C. R., and G. Franceschini. 1988. Effects of fibrates on serum lipids and atherosclerosis. *Pharmacol. Ther.* **37**: 167–191.
- Einarsson, K., S. Ericsson, S. Ewerth, E. Reihner, M. Rudling, D. Stahlberg, and B. Angelin. 1991. Bile acid sequestrants: mechanisms of action on bile acid and cholesterol metabolism. *Eur. J. Clin. Pharmacol.* **40**: S53–58.
- Gotto, A. M. 1993. Dyslipidemia and atherosclerosis. A forecast of pharmaceutical approaches. *Circulation.* **87**: III54–59.

5. Steinberg, D. 1986. Studies on the mechanism of action of probucol. *Am. J. Cardiol.* **57**: 16H–21H.
6. Matsuda, K. 1994. ACAT inhibitors as antiatherosclerotic agents: compounds and mechanisms. *Med. Res. Rev.* **14**: 271–305.
7. Tanaka, H., and T. Kimura. 1994. ACAT inhibitors in development. *Exp. Opin. Invest. Drugs.* **3**: 427–436.
8. Suckling, K. E., and E. F. Stange. 1985. Role of acyl-CoA:cholesterol acyltransferase in cellular cholesterol metabolism. *J. Lipid Res.* **26**: 647–671.
9. Bell, F. P. 1986. Arterial cholesterol esterification by acyl CoA:cholesterol acyltransferase: its possible significance in atherogenesis and its inhibition by drugs. In *Pharmacological Control of Hyperlipidaemia*. R. Fears, R. I. Levy, J. Shepard, C. J. Packard, and N. E. Miller, editors. J. R. Prous Science Publishers, Spain. 409–422.
10. Sliskovic, D. R., and A. D. White. 1991. Therapeutic potential of ACAT inhibitors as lipid lowering and anti-atherosclerotic agents. *Trends Pharmacol. Sci.* **12**: 194–199.
11. Bocan, T. M. A., S. B. Mueller, P. D. Uhlendorf, R. S. Newton, and B. R. Krause. 1991. Comparison of CI-976, an ACAT inhibitor, and selected lipid-lowering agents for antiatherosclerotic activity in iliac-femoral and thoracic aortic lesions: *Atheroscler. Thromb.* **11**: 1830–1843.
12. Tanaka, H., I. Ohtsuka, M. Kogushi, T. Kimura, T. Fujimori, T. Saeki, K. Hayashi, H. Kobayashi, T. Yamada, H. Hiyoshi, and I. Saito. 1994. Effect of the acyl-CoA:cholesterol acyltransferase inhibitor, E5324, on experimental atherosclerosis in rabbits. *Atherosclerosis.* **107**: 187–210.
13. Schnitzer-Polokoff, R., D. Compton, G. Boykow, H. Davis, and R. Burrier. 1991. Effects of acyl-CoA:cholesterol O-acyltransferase inhibition on cholesterol absorption and plasma lipoprotein composition in hamsters. *Comp. Biochem. Physiol.* **99A**: 665–670.
14. Sugiyama, Y., E. Ishikawa, H. Odaka, N. Miki, H. Tawada, and H. Ikeda. 1995. TMP-153, a novel ACAT inhibitor, inhibits cholesterol absorption and lowers plasma cholesterol in rats and hamsters. *Atherosclerosis.* **13**: 71–78.
15. Krause, B. R., R. F. Bousley, K. A. Kieft, and R. L. Stanfield. 1992. Effect of the ACAT inhibitor CI-976 on plasma cholesterol concentrations and distribution in hamsters fed zero- and low-cholesterol diets. *Clin. Biochem.* **25**: 371–377.
16. Largis, E. E., C. H. Wang, V. G. DeVries, and S. A. Schaffer. 1989. CL 277,082: a novel inhibitor of ACAT-catalyzed cholesterol esterification and absorption. *J. Lipid Res.* **30**: 681–690.
17. Harris, W. S., C. A. Dujovne, K. von Bergmann, J. Neal, J. Akester, S. L. Windsor, D. Greene, and Z. Look. 1990. Effects of the ACAT Inhibitor CL 277,082 on cholesterol metabolism in humans. *Clin. Pharmacol. Ther.* **48**: 189–194.
18. Hainer, J. W., J. G. Terry, J. M. Connell, H. Zyruk, R. M. Jenkins, D. L. Shand, P. J. Gillies, K. J. Livak, T. L. Hunt, and J. R. Crouse. 1994. Effect of the acyl-CoA:cholesterol acyltransferase inhibitor DuP 128 on cholesterol absorption and serum cholesterol in humans. *Clin. Pharmacol. Ther.* **56**: 65–74.
19. Catapano, A. L. 1992. Mode of action of fibrates. *Pharmacol. Res.* **26**: 331–340.
20. Lalezari, I., S. Rahbar, P. Lalezari, G. Fermi, and M. F. Perutz. 1988. LR16, a compound with potent effects on the oxygen affinity of hemoglobin, on blood cholesterol, and on low density lipoprotein. *Proc. Natl. Acad. Sci. USA.* **85**: 6117–6121.
21. Hudson, K., S. Mojumder, and A. J. Day. 1983. The effect of bezafibrate and clofibrate on cholesterol ester metabolism in rabbit peritoneal macrophages stimulated with acetylated low density lipoproteins. *Exp. Molec. Pathol.* **38**: 77–81.
22. Reddy, J. K., and N. D. Lalwai. 1983. Carcinogenesis by hepatic peroxisome proliferators: evaluation of the risk of hypolipidemic drugs and industrial plasticizers to humans. *Crit. Rev. Toxicol.* **12**: 1–58.
23. Aoyama, T., J. P. Hardwick, S. Imaoka, Y. Funae, H. V. Gelboin, and F. J. Gonzalez. 1990. Clofibrate-inducible rat hepatic P450s IVA1 and IVA3 catalyze the omega- and (omega-1)-hydroxylation of fatty acids and the omega-hydroxylation of prostaglandins E1 and F2 alpha. *J. Lipid Res.* **31**: 1477–1482.
24. Chapman, J. M., R. L. Hawke, K. W. Franzmann, and K. J. O'Connor. 1992. Anti-atherosclerotic Aryl Compounds. W09201468 (920625 with Univ. South Carolina), Burroughs Wellcome.
25. Mor, G., and N. Lichtenstein. 1970. Inhibitors of rat liver glutaminase. *Israel J. Chem.* **8**: 595–601.
26. Lake, B., G., T. J. B. Gray, C. R. Stubberfield, J. A. Beaman, and S. D. Gangolli. 1983. Induction of lauric acid hydroxylation and maintenance of cytochrome P-450 content by clofibrate in primary cultures of rat hepatocytes. *Life Sci.* **33**: 249–254.
27. Heider, J. G., C. E. Pickens, and L. A. Kelly. 1983. Role of acyl-CoA:cholesterol acyltransferase in cholesterol absorption and its inhibition by 57-118 in the rabbit. *J. Lipid Res.* **24**: 1127–1134.
28. Sedmak, J. J., and S. E. Grossberg. 1977. A rapid, sensitive, and versatile assay for protein using Coomassie Brilliant Blue G250. *Anal. Biochem.* **79**: 544–552.
29. Lalezari, L., and P. Lalezari. 1989. Synthesis and investigation of effects of 2-[4-[(arylamino)carbonyl]amino]phenoxy]-2-methylpropionic acids on the affinity of hemoglobin for oxygen: structure–activity relationships. *J. Med. Chem.* **32**: 2352–2357.
30. DeVries, V. G., S. A. Schaffer, E. E. Largis, M. D. Dutia, C. H. Wang, J. D. Bloom, and A. S. Katocs, Jr. 1986. An acyl-CoA:cholesterol O-acyltransferase inhibitor with hypocholesterolemic activity. *J. Med. Chem.* **29**: 1131–1133.
31. De Vries, V. G. 1986. Antiatherosclerotic ureas and thio-ureas. U.S. Patent No. 4,623,662, American Cyanamid Company.
32. Abshagen, U., W. Bablok, K. Koch, P. D. Lang, H. A. E. Schmidt, M. Senn, and H. Stork. 1979. Disposition pharmacokinetics of bezafibrate in man. *Eur. J. Clin. Pharmacol.* **16**: 31–38.
33. Woolf, T. F., S. M. Bjorge, A. E. Black, A. Holmes, and T. Chang. 1991. Metabolism of the acyl-CoA:cholesterol acyltransferase inhibitor 2,2-dimethyl-N-(2,4,6-trimethoxyphenyl)dodecanamide in rat and monkey. *Drug Metab. Dispos.* **19**: 696–702.
34. Hirohashi, A., A. Nagat, H. Miyawaki, H. Nakatani, and K. Toki. 1976. Metabolism of linoleamides I. Absorption, excretion, and metabolism of N-( $\alpha$ -methylbenzyl)linoleamide in rat and man. *Xenobiotica.* **6**: 329–337.
35. Fahimi, H. D., A. Reinicke, M. Sujatta, S. Yokota, M. Ozel, F. Hartig, and K. Stegmeier. 1982. The short- and long-term effects of bezafibrate in the rat. *Ann. N.Y. Acad. Sci.* **386**: 111–113.
36. Watanabe, T., M. Mitsukawa, S. Horie, T. Suga, and K. Seki. 1987. Effects of some hypolipidemic agents on biochemical values and hepatic peroxisomal enzymes in rats: comparison of probucol, CGA, KCD-2332, MLM-160, AL-369 and clonofibrate with clofibrate. *J. Pharmacobio-Dyn.* **10**: 142–147.

37. Azarnoff, D. L., J. K. Reddy, C. Hignite, and T. Fitzgerald. 1975. Structure activity relationships of clofibrate-like compounds on lipid metabolism. In Proceedings VI Int. Congress of Pharmacology. H. Vapaatalo, editor. IUPHAR, Helsinki. Vol. 4: 137–147.
38. Esbenshade, T. A., V. S. Kamanna, H. A. I. Newman, V. Tortorella, D. T. Witiak, and D. R. Feller. 1990. In vivo and in vitro peroxisome proliferation properties of selected clofibrate analogues in the rat. *Biochem. Pharmacol.* **40**: 1263–1274.
39. Eason, C. T., P. Powles, G. Henry, A. J. Spencer, A. Pattison, and F. W. Bonner. 1989. The comparative pharmacokinetics and gastric toxicity of bezafibrate and ciprofibrate in the rat. *Xenobiotica.* **19**: 913–925.
40. Green, S., and W. Wahli. 1994. Peroxisome proliferator-activated receptors: finding the orphan a home. *Mol. Cell. Endocrinol.* **100**: 149–153.
41. Desvergne, B., and W. Wahli. 1995. PPAR: a key nuclear factor in nutrient/gene interactions? *Inducible Gene Expression.* **1**: 142–176.
42. Kliewer, S. A., J. M. Lenhard, T. M. Willson, I. Patel, D. C. Morris, and J. M. Lehmann. 1995. A prostaglandin J<sub>2</sub> metabolite binds peroxisome proliferator-activated receptor gamma and promotes adipocyte differentiation. *Cell.* **83**: 813–819.
43. Forman, B. M., P. Tontonoz, J. Chen, R. P. Brun, B. M. Spiegelman, and R. M. Evans. 1995. 15-Deoxy-delta 12, 14-prostaglandin J<sub>2</sub> is a ligand for the adipocyte determination factor PPAR gamma. *Cell.* **83**: 803–812.
44. Lehmann, J. M., L. B. Moore, T. A. Smith-Oliver, W. O. Wilkison, T. M. Willson, and S. A. Kliewer. 1995. An anti-diabetic thiazolidinedione is a high affinity ligand for peroxisome proliferator-activated receptor  $\gamma$  (PPAR $_{\gamma}$ ). *J. Biol. Chem.* **270**: 12953–12956.
45. Willson, T. M., J. E. Cobb, D. J. Cowan, R. W. Wiethe, I. D. Correa, S. R. Prakash, K. D. Beck, L. B. Moore, S. A. Kliewer, and J. M. Lehmann. 1996. The structure-activity relationship between peroxisome proliferator-activated receptor gamma agonism and the antihyperglycemic activity of thiazolidinediones. *J. Med. Chem.* **39**: 665–668.
46. Aldridge, T. C., J. D. Tugwood, and S. Green. 1995. Identification and characterization of DNA elements implicated in the regulation of CYP4A1 transcription. *Biochem. J.* **306**: 473–479.
47. Palmer, C. N., M. H. Hsu, A. S. Muerhoff, K. J. Griffin, and E. F. Johnson. 1994. Interaction of the peroxisome proliferator-activated receptor alpha with the retinoid X receptor alpha unmasks a cryptic peroxisome proliferator response element that overlaps an ARP-1-binding site in the CYP4A6 promoter. *J. Biol. Chem.* **269**: 18083–18089.
48. Muerhoff, A. S. 1992. The peroxisome proliferator-activated receptor mediates the induction of CYP4A6, a cytochrome P450 fatty acid omega-hydroxylase, by clofibrate acid. *J. Biol. Chem.* **267**: 19051–19053.
49. Gonzalez, F. J., and D. W. Nebert. 1990. Evolution of the P450 gene superfamily: animal-plant 'warfare', molecular drive and human genetic differences in drug oxidation. *Trends Genet.* **6**: 182–186.
50. Nelson, D. R., T. Kamataki, D. J. Waxman, P. Guengerich, R. W. Estabrook, R. Feyereisen, F. J. Gonzalez, M. J. Coon, I. C. Gunslaus, O. Gotoh, K. Okuda, and D. W. Nebert. 1993. The P450 superfamily: update on new sequences, gene mapping, accession numbers, early trivial names of enzymes, and nomenclature. *DNA Cell Biol.* **12**: 1–15.
51. Kawashima, H., E. Kusunose, Y. Kikuta, H. Kinoshita, S. Tanaka, S. Yamamoto, T. Kishimoto, and M. Kusunose. 1994. Purification and cDNA cloning of human liver CYP4A fatty acid  $\omega$ -hydroxylase. *J. Biochem.* **116**: 74–80.
52. Stael, B., N. Vu-Dac, V. A. Kosykh, R. Saladin, J.-C. Fruchart, J. Dallongeville, and J. Auwerx. 1995. Fibrates downregulate apolipoprotein C-III expression independent of induction of peroxisomal acyl coenzyme A oxidase. *J. Clin. Invest.* **95**: 705–712.
53. Hertz, R., J. Bishara-Shieban, and J. Bar-Tana. 1995. Mode of action of peroxisome proliferators as hypolipidemic drugs: suppression of apolipoprotein C-III. *J. Biol. Chem.* **270**: 13470–13475.
54. Haubenwallner, S., A. D. Essenburg, B. C. Barnett, M. E. Pape, R. B. DeMattos, B. R. Krause, L. L. Minton, B. J. Auerbach, R. S. Newton, T. Leff, and C. L. Bisgaier. 1995. Hypolipidemic activity of select fibrates correlates to changes in hepatic apolipoprotein C-III expression: a potential physiologic basis for their mode of action. *J. Lipid Res.* **36**: 2541–2551.
55. Sirtori, C. R., L. Calabresi, J. P. Werba, and G. Franceschini. 1992. Tolerability of fibric acids. Comparative data and biochemical bases. *Pharmacol. Res.* **26**: 243–260.
56. Cayen, M. N. 1985. Disposition, metabolism and pharmacokinetics of antihyperlipidemic agents in laboratory animals and man. *Pharmacol. Ther.* **29**: 157–204.
57. Abshagen, U., S. Sporn-Radun, and J. Marinow. 1980. Steady-state kinetics of bezafibrate and clofibrate in healthy female volunteers. *Eur. J. Clin. Pharmacol.* **17**: 305–308.
58. Wanner, C., H. Wieland, P. Schollmeyer, and W. H. Horl. 1991. Beclobrate: pharmacodynamic properties and therapeutic use in hyperlipidemia. *Eur. J. Clin. Pharmacol.* **40**: S85–S89.
59. Davison, C., D. Benziger, A. Fritz, and J. Edelson. 1975. Absorption and disposition of 2-[4-(2,2-dichlorocyclopropyl)phenoxy]-2-methylpropanoic acid, Win 35,833, in rats, monkeys, and men. *Drug Metab. Disp.* **3**: 520–524.